

CALCULATION OF INJECTION AND EXTRACTION ORBITS FOR THE IPCR SSC

A. Goto, Y. Yano, N. Kishida, N. Nakanishi and T. Wada

The Institute of Physical and Chemical Research, Wako-shi, Saitama 351, Japan

Abstract.— Calculations of beam trajectories in the injection and extraction systems for the IPCR SSC were done and the characteristics of those elements were determined. Beam centering at injection and off-centering for single turn extraction by use of first harmonic fields were also studied. The rather simple conditions at the injection point for a well-centered acceleration orbit are also discussed.

1. Introduction.— In designing injection and extraction system it is fundamental to calculate beam trajectories in those systems in detail. For this purpose, we have developed computer programs for the numerical orbit calculation in which the measured field data are used and the acceleration is considered. The characteristics of the injection and extraction elements have been determined with the aid of these programs. Layout of those elements is shown in figure 1 of the paper reported at this conference¹⁾.

A beam can be non-centered in the injection region for different reasons, i.e. the undershoot fields of injection elements, the non-optimal position and field strength of electrostatic inflection channel and so on. In the extraction region the beam separation due to acceleration is not adequate for some of the high energy and low mass beams (e.g. $^{12}\text{C}^{6+}$; 134 MeV/u). The magnetic field perturbation is then required to center the non-centered beam and enhance the turn spacing for single turn extraction. The behaviors of the beam in the presence of the first harmonic field were studied.

It is important, especially for a variable energy and multiparticle cyclotron like the IPCR SSC, to accelerate the beam along a well-centered acceleration orbit. The rather simple conditions at the injection point have been found to give good results.

In this paper we describe the calculations of the injection and extraction orbits together with centering at injection and off-centering for single turn extraction for the IPCR SSC by using the numerical orbit calculation programs. We also discuss the conditions of a well-centered acceleration orbit.

2. Injection orbit.— In order to get a beam of good quality some conditions should be imposed upon the beam at the injection point^{1),2)}. Beam trajectories were calculated so that the beam fulfilled the optimal conditions of a well-centered acceleration orbit and matched to the eigen-ellipse of the SSC.

The characteristics of the newly-developed program code (INJECT) are as follows³⁾:

- The motion of charged particles in electro-magnetic fields is calculated with time as the independent variable.
- The fields of each injection element can be superimposed onto that of the sector magnets (base

field) at arbitrary positions.

- It can deal with the acceleration by the electric field in the dee gaps.
- It can calculate individually the paths of 17 particles consisting of a central particle and two groups of 8 particles describing phase ellipses in both (r, r') and (z, z') phase spaces.

In the calculation we chose three typical kinds of particles, i.e. 0.84 MeV/u $^{238}\text{U}^{40+}$, 7 MeV/u $^{12}\text{C}^{6+}$ and 4 MeV/u $^{12}\text{C}^{6+}$. The turn separations of the first two are the largest and smallest ones, respectively, while that of the third is in the middle of them. The field data used are as follows: The base fields are the isochronous fields for each particle beam, which were calculated on the basis of the field data of the 1/4-scale model magnet⁴⁾. The magnetic field of BML is that of the 1/1-scale model bending magnet. For the fields of MICs and EIC we adopted the analytic expression for fringe field ("the extended fringing field")⁵⁾. These fields of the injection elements were superimposed onto the base field in desired regions. The procedure of the calculations is as follows: At a starting point (the exit of EIC) we put a beam having an energy to some extent higher than its injection energy from the pre-accelerator, lying on the corresponding well-centered acceleration orbit and matching to the eigen-ellipse of the SSC. Then with these initial conditions the beam was traced backward from there through MICs up to the entrance of BML. The beam got "deceleration" in the dee gaps on the way. The positions and bending powers etc. of EIC, MIC1 and MIC2 were adjusted so that the beam cleared the aperture of BML, which was fixed at the proper position. If the "final" energy at the entrance of BML deviated from the injection energy submitted from the pre-accelerator, the energy at the starting point was varied correspondingly and the beam was traced again from the beginning. This procedure was repeated until all these conditions were fulfilled. The beam were traced further along the acceleration orbit to check the magnitudes of beam separations in the vicinity of the injection elements.

An example of the calculated beam trajectories is shown in figure 1. The characteristics of EIC, MIC1, MIC2 and BML thus determined are listed in Table 1 of Ref. 1. It was found that MIC1 and MIC2 can be fixed but EIC should be radially adjustable by 15 mm. It was also found that the beam separations of 36 mm at the exit of MIC1 and 19 mm at that of EIC can be obtained

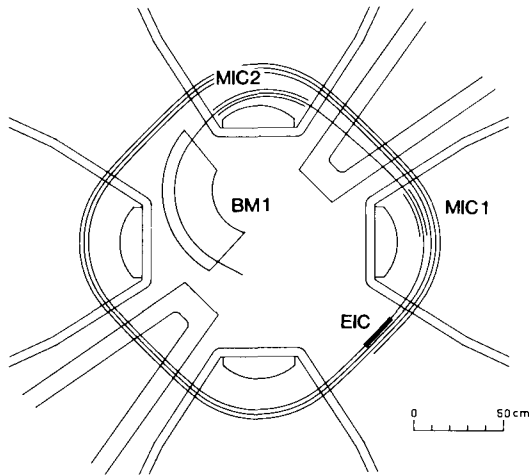


Fig. 1 : Injection orbit through the injection elements and the first few well-centered acceleration orbits for 7 MeV/u $^{12}\text{C}^{6+}$ beam.

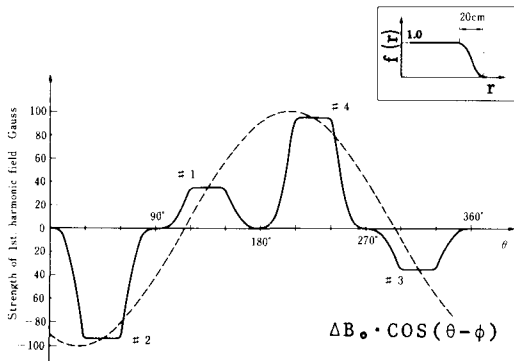


Fig. 2 : Angular distributions of the first harmonic field used in the calculation (solid line). Its radial distributions are shown in the inset. Leave the details to the text.

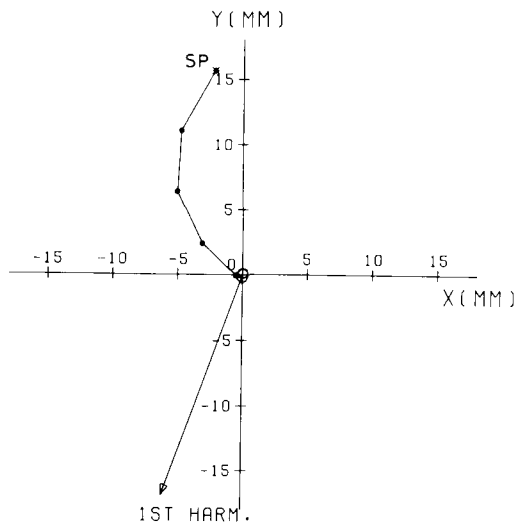


Fig. 3 : Motion of the orbit center for centering of 0.84 MeV/u $^{238}\text{U}^{40+}$ beam. The strength and angle of the first harmonic field are 24 Gauss and 250° , respectively. The exit of EIC is positioned in the direction of x axis. SP stands for the starting point of the orbit center.

even in the severest case. These beam separations assure the accelerated beam not to hit these elements.

It may be rather difficult in fact to choose optimal settings of these elements for a well-centered acceleration orbit because a quantity R'_{inj} , for example, is very sensitive to these setting parameters. Furthermore the undershoot fields of the elements can cause the off-centering of a beam. We have then studied the behaviours of the beams in the presence of first harmonic fields using the code INJHARM, the essential function of which is the same as that of the code INJECT, and determined the parameters of the harmonic coils to center the non-centered beam.

The value of a first harmonic field at a point (r, θ) is given by

$$\Delta B^i(r, \theta) = \Delta B_O^i \cdot \{B_{iso}(r, \theta) / B_{iso}^h(R_c)\} \cdot f(r), \quad (1)$$

where i stands for the sector magnet number, $B_{iso}(r, \theta)$ is the isochronous field at the point and $B_{iso}^h(R_c)$ is that at the hill center where the harmonic coil exists. $f(r)$ is the normalized radial distribution of the harmonic field. A Fermi type distribution with 20 cm width is assumed. The radial position of half maximum of this distribution is assumed to vary along a Gordon trajectory. ΔB_O^i is given by

$$\Delta B_O^i = \Delta B_O \cos(\theta_i - \phi), \quad (2)$$

for the magnitude and direction of the first harmonic field ΔB_O and ϕ , respectively. Here θ_i is the azimuth of the hill of the i -th sector magnet when that of the injection point is assumed to be 0° . The distributions of the first harmonic field are shown schematically in figure 2.

This field was superimposed onto the base field and the motion of orbit center^(6),7) was calculated in those fields. In the calculation a off-centered beam was artificially given by putting the beam onto its equilibrium orbit at the injection point.

It was found to be necessary for one to divide all kinds of particles into three parts according to turn separations and to center them respectively by three sets of harmonic coils. It was found to be optimum that these sets of coils be placed at R_h (the radial position at the hill center) = 101.5, 113.5 and 125.5 cm, respectively. They are set along Gordon trajectories and also used as trim coils. Figure 3 presents calculators for the motion of the orbit center of the $^{238}\text{U}^{40+}$ beam. The orbit center starting at the position about 15 mm apart from the machine center is centered after about five particle revolutions. In this case a field of 24 Gauss needed to be generated by the most outside set of harmonic coils.

3. Extraction orbit. - The beam separation of low-energy light ions and heavy ions due to acceleration is large enough for single turn extraction. For high energy light ions this separation is not adequate, so that the magnetic field perturbation will be required to enlarge the beam separation at the extraction point. We use the first harmonic field for this purpose⁽⁶⁾. Furthermore we aim to extract the beam before $\nu_r=1$ resonance in order to avoid the degradation of the beam emittance. The study was concentrated to the extraction of the 134 MeV/u (the injection energy is 7 MeV/u) $^{12}\text{C}^{6+}$ beam whose beam separation is smallest and whose magnetic

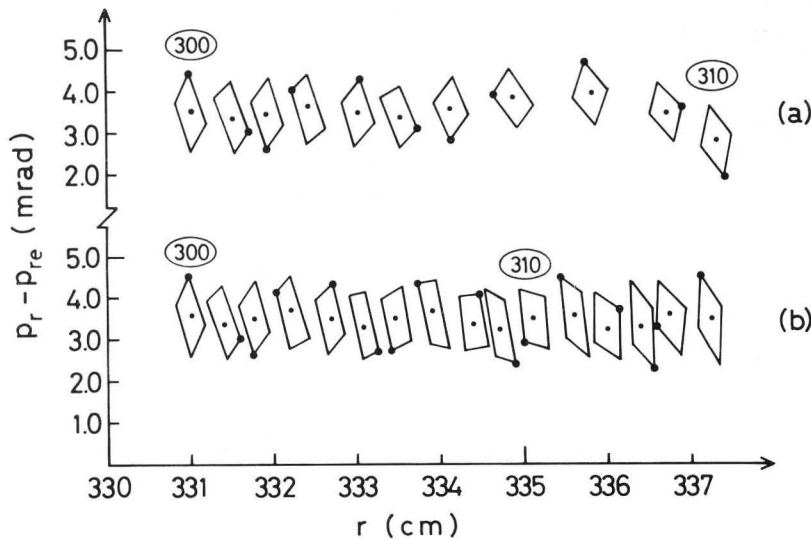


Fig. 5 : Radial phase space envelopes for 134 MeV/u $^{12}\text{C}^{6+}$ beam near extraction; a) with and b) without the first harmonic field. The numbers refer to the revolutions of the beam. Beam emittance is taken to be 20 mm·mrad.

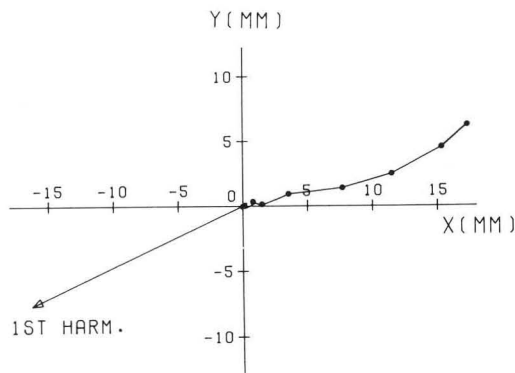


Fig. 4 : Motion of the orbit center for off-centering of 134 MeV/u $^{12}\text{C}^{6+}$ beam. The strength and angle of the first harmonic field are 100 Gauss and 205°, respectively. The entrance of EDC is positioned at about 15°.

rigidity is largest among the accelerated particles.

At first the well-centered acceleration orbit of the 134 MeV/u $^{12}\text{C}^{6+}$ beam was calculated from the injection point up to near extraction region using the code ACCEL. Then the motion of orbit center of this beam before extraction was studied in the presence of the first harmonic field and its parameters were determined so as to enlarge the beam separation at the entrance of EDC. This was made using the code EXTHARM. Finally with the code EXTRACT was calculated the extraction orbit from the entrance of EDC through MDC1, MDC2 and EBM1 up to the exit of EBM2. In this calculation the beam was traced further backward along the acceleration orbit to check the beam separation between the extraction and the last acceleration orbits. The functions of the codes EXTRACT and EXTHARM are almost the same as those of the codes INJECT and INJHARM, respectively.

Figure 4 presents calculations for the motion of orbit center of the 134 MeV/u $^{12}\text{C}^{6+}$ beam. As can be seen in this figure the orbit center moves from the machine center toward the entrance of EDC (which is

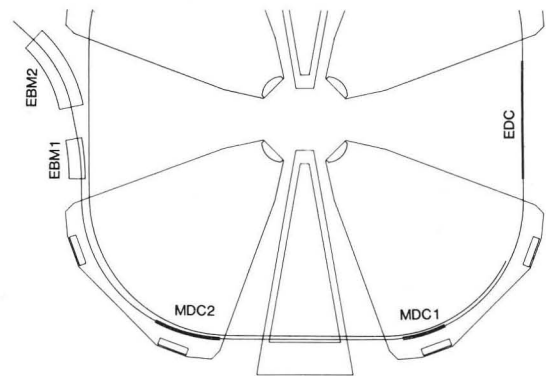


Fig. 6 : Extraction orbit through the extraction elements and the last acceleration orbit for 134 MeV/u $^{12}\text{C}^{6+}$ beam.

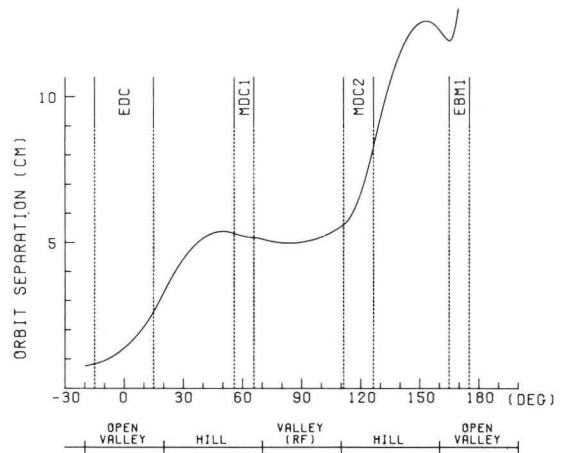


Fig. 7 : Orbit separation between the extraction and the last acceleration orbits as a function of azimuth position.

placed at about 15°) by steps of maximum 5 mm. In this case the direction and strength of the first harmonic field are 205° and 100 Gauss, respectively. It was found to be optimum that coils be placed at $R_h = 372$ cm, while the radius of the last turn at hill center is 373 cm. A field of 100 Gauss is considerably large, but

this is feasible enough for these coils. In figure 5 are shown the beam phase spaces with and without the first harmonic field. It can be seen that the beams which were contact with each other are separated with the first harmonic field by about 5 mm at the extraction point. The septum of EDC is located between 308 and 309 revolutions. The degradation of the beam emittance cannot be seen at all during this process. Figure 6 presents the extraction orbit together with the configuration of the elements. Figure 7 shows the beam separation between the extraction and the last acceleration orbits. This is large enough to place each element not to disturb the last acceleration orbit. The characteristics of EDC, MDC1, MDC2, EBM1 and EBM2 thus determined are listed in Table 1 of Ref. 1. The extractions of other particles are now being studied.

4. Beam centering. - In order that the well-centered acceleration orbit can be realized, a particle has to move in the SSC as shown in figure 8. The essential feature of this motion is that the particle crosses the equilibrium orbit (E.O.) corresponding to its kinetic energy with an appropriate divergence every time it reaches the mid-line of open valley, e.g. points A and D. $R(i)$ and $R(i+1)$ represent the radial distance measured from the machine center to the i -th and $(i+1)$ -th E.O., respectively. If we used a single-gap acceleration system, the particle would reach the point B and leave the same point after it gains the energy. In our double-gap acceleration system, however, the particle is deflected by the accel. gap 1 and then is inflected by the accel. gap 2 as shown in the inset. Because these deflection and inflection angles are almost the same, the treatment of this double-gap acceleration process can be simplified by describing the process in such a way that the particle reaches the point B and then leaves the point C after it gains the energy which is to be obtained by the passage of two acceleration gaps. The radial shift of the point C from the point B is given by $\epsilon(i)$.

Now let us consider the motion of the well-centered particle mentioned above on radial phase space. The facts that eigen-ellipses for a certain E.O. given at mid-lines of four valleys (including dee valleys) are identical and that they are erect ellipses make the description so simpler. We can transform these ellipses into circular shapes by multiplying certain appropriate scaling factor to the values of angular divergence. This scaling factor is given by r_0/r'_0 , where r_0 (radial displacement) and r'_0 (angular divergence) represent the principal axes of ellipse.

Figure 9 shows the diagram describing the motion of the well-centered particle on radial phase space. The left (right) vertical axis (R') gives the angular divergence for the i -th ($(i+1)$ -th) E.O. which is properly scaled. The horizontal axis (R) gives the radial distance from the machine center to the E.O. of interest at the valley mid-lines. This axis is common to all the E.O. considered. The particle which leaves the point A with the energy of $E(i)$ and the angular divergence of $a(i)$ moves along the circular arc AB and reaches the point B. Then it gets the energy gain of $\Delta E = E(i+1) - E(i)$ and the radial shift of $\epsilon(i)$ by the acceleration system. After this acceleration process the particle moves along the circular arc CD and reaches the point D. $v(i)$ and $v(i+1)$ represent the radial betatron frequencies for the i -th and $(i+1)$ -th E.O., respectively. Strictly speaking, the point C should be repositioned according to the difference of scaling factors for the i -th and $(i+1)$ -th E.O. This, however, is minor correction as long as the turn

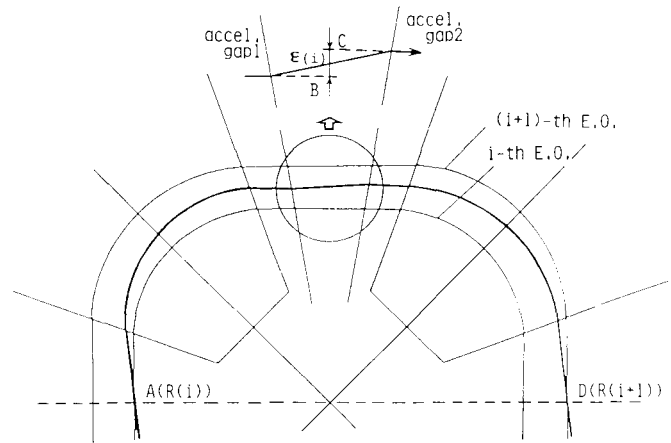


Fig. 8 : Well-centered acceleration orbit (thick solid line). A particle moves clockwise and is accelerated by a couple of gaps in one dee (see the inset). The i -th and $(i+1)$ -th equilibrium orbits are also indicated. Leave the details to the text.

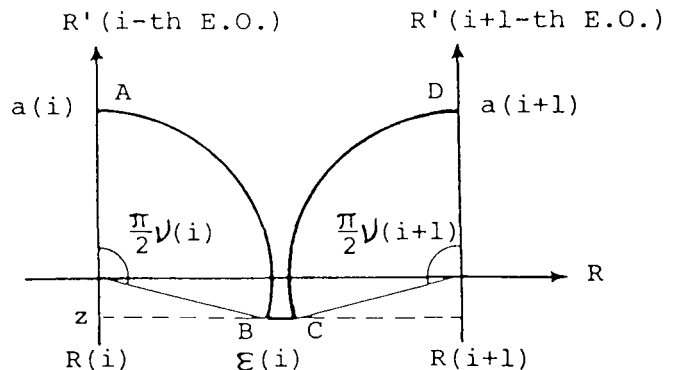


Fig. 9 : Diagram describing motion of a well-centered particle on radial phase space. Points (A-D) corresponds to those in figure 8. Leave the details to the text.

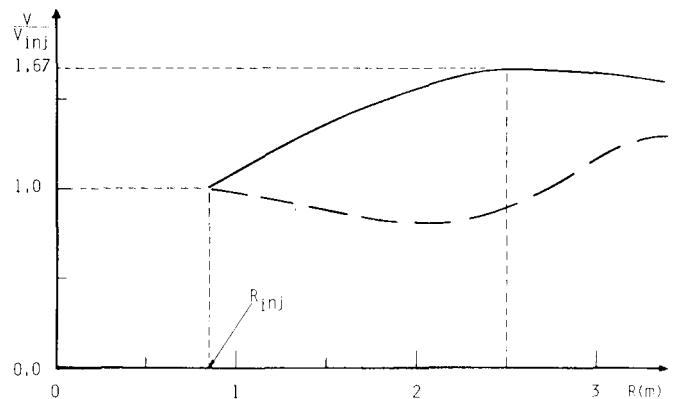


Fig. 10 : Radial distribution of RF voltage used in the calculations of beam centering of $^{12}\text{C}^{6+}$ with injection energy of 50.57 MeV. R represents the distance measured along the mid-line of dee gap from the machine center. The RF voltage is normalized by the voltage at the position (R_{inj}) of the first acceleration orbit.

The dashed line shows the voltage distribution obtained by the present structure of RF resonator and the solid line the resultant distribution calculated so that the centering equation can hold throughout the acceleration region of the SSC.

separation is not very large.

From the diagram shown in figure 9, we can formulate the expression (which will be called "centering equation") for getting the well-centered acceleration orbit. This equation resulted in the form of

$$-z \left\{ \frac{1}{\tan((\pi/2)(v(i)-1))} + \frac{1}{\tan((\pi/2)(v(i+1)-1))} \right\} + \epsilon(i) = R(i+1) - R(i), \quad (3)$$

where z is indicated in the diagram. We assume that the trajectory between a couple of acceleration gaps can be approximated by a straight line and that it cuts the mid-line of dee valley at right angle. This is a fairly good assumption because the magnetic field in the dee valley region is very low. Further, we assume that the particle crosses the mid-line of dee valley at the moment the RF voltage becomes null. Then we can get the following expressions.

$$\Delta E = 2g^{(1)} qV(R^* \sec(\theta_{dee}/2)) \sin(\Delta\theta) / \Delta\theta \quad (4)$$

$$\Delta\theta = g^{(2)} / R^* \quad (5)$$

$$\epsilon(i) = g^{(3)} (\Delta E / 2E(i)) R^* \quad (6)$$

$$R = R(i) + a(i) \sin((\pi/2)v(i)) \quad (7)$$

$$z = a(i) \cos((\pi/2)v(i)). \quad (8)$$

$g^{(1)}$, $g^{(2)}$ and $g^{(3)}$ are given by using the geometrical parameters for the sector magnet and RF resonator systems and the harmonic number of acceleration. q is the charge number of the particle, θ_{dee} the dee angle and $V(x)$ the RF voltage with respect to the distance measured along the mid-line of dee gap from the machine center. The term of $\sin(\Delta\theta)/\Delta\theta$ in eq. 4 is introduced by the transit-time effect due to the finite acceleration gap.

At first, we use the centering equation in order to determine the conditions for centering the injected beam. The central particle must be injected at the

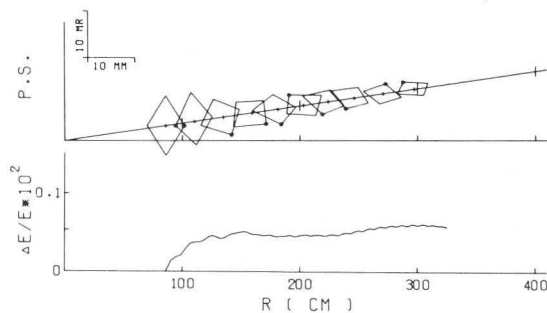


Fig. 11 : Transformation of beam properties (radial emittance and energy resolution) calculated at the mid-line of open valley. Calculations were made by using the RF voltage distribution given by the dashed line in figure 10.

References

- 1) Y. Yano et al., "Beam injection and extraction system for the IPCR SSC", this conference.
- 2) N. Kishida et al., "Beam transport system for the IPCR SSC", this conference.
- 3) A. Goto et al., Sci. Papers I.P.C.R., 74 (1980) 124
- 4) N. Nakanishi et al., IPCR Cyclotron Progr. Rep., 13, (1979) 12.
- 5) H.A. Enge, Rev. Sci. Instr., 35 (1964) 278.

radial position of $R(1)$ with the appropriate RF phase. This phase can be calculated by the first-order transformation matrix theory. Assuming that $v(1)=v(2)$ and $R^*=R(1)$, the expression to get the necessary angular divergence a (in actual unit) at injection point is obtained from eq. 3. This is written by

$$a^* = \{R(2) - R(1) - \epsilon(1)\} (r_0' / r_0) / \{2 \sin((\pi/2)v(1))\}. \quad (9)$$

The right-hand side of eq. 9 can be calculated from the isochronous field data and given RF voltage distribution of $V(x)$.

The calculation of beam centering of $^{12}C^{6+}$ with injection energy of 50.57 MeV was made as an example. We used the same isochronous field data as in sections 2 and 3 and the RF voltage distribution shown in figure 10. The voltage at R_{inj} was taken to be 250 kV. The fairly good result was obtained that the orbit center is injected onto the circle of radius of about 0.3 mm. Figure 12 shows the transformation of beam properties with the radius given by tracing 4 particles together with the central particle numerically. These 4 particles exist on the eigen-ellipse of emittance of 20 mm.mrad at injection point. The CP phase matching⁸⁾ is made. The alternating magnetic field⁹⁾ induced by the radial distribution of RF voltage is also taken into account.

Secondly, we calculated the RF voltage distribution which makes the centering equation hold throughout the acceleration region of the SSC. This distribution can be obtained by solving eq. 3 iteratively by use of eqs. 4-8 and the isochronous field data. The resultant RF voltage distribution is shown in figure 10. In this case, the orbit center moves along the circle of radius of about 0.1 mm. Figure 12 shows the transformation of beam properties calculated by using the desired distribution. It can be seen that the energy resolution and the beam emittance at extraction point are improved considerably.

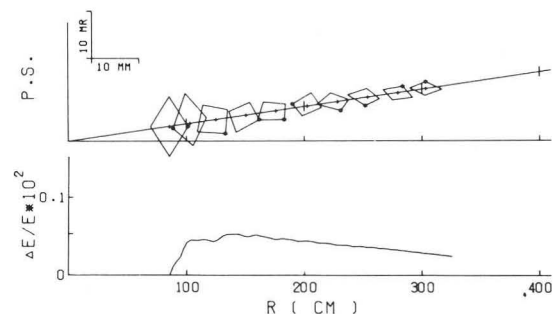


Fig. 12 : Transformation of beam properties. Calculations were made by using the RF voltage distribution given by the solid line in figure 10.

- 6) H.L. Hagedoorn and N.F. Verster, Nucl. Instr. Meth., 18/19 (1962) 201
- 7) J.M. Nieuwland, "Extraction of particles from a compact isochronous cyclotron", Thesis 1973, Eindhoven.
- 8) W.M. Schulte, "The theory of accelerated particles in AVF cyclotrons", Thesis 1978, Eindhoven.
- 9) W. Joho, Particle Accelerators, 6 (1974) 41.